Evaluation of Bending Strength of Carburized Gears

Tomoya Masuyama, Katsumi Inoue, Masashi Yamanaka, Kenichi Kitamura and Tomoyuki Saito

Management Summary

The aim of our research is to clearly show the influence of defects on the bending fatigue strength of gear teeth. Carburized gears have many types of defects, such as non-martensitic layers, inclusions, tool marks, etc. It is well known that high strength gear teeth break from defects in their materials, so it's important to know which defect limits the strength of a gear.

In this article, we propose a method of inferential identification of principal defects and an evaluation of strength based on defect size. Furthermore, the results of this research should show how to reduce the defects.

Table 1—Dimensions of test gears used for the derivation of a formula.

Code		C1	C2	EP1	EP2
Module	[mm]		5		
Number of teeth			18		
Face width	[mm]		8		
Material			SCM415		
Heat treatment			Carburized		
Removal stock	[μm]	0	0	10	20
Surface residual stress	[MPa]	−230	−130	−160	−190
Fatigue strength	[MPa]	842	890	901	906

Figure 1—Strength of electropolished gear with a micronotch.

Abstract

The high load capacity of carburized gears mainly originates from the hardened layer and induced residual stress. On the other hand, the decarburization at the surface, which causes a nonmartensitic layer, and the inclusions such as oxides and segregation act as a latent defect, and the defect considerably reduces the fatigue strength. In this connection, the authors have proposed a formula of strength evaluation by separately quantifying the influence of the defect. However, the principal defect that limits the strength of gears that have several kinds of defects remains unclarified. This paper presents a method of inferential identification of the principal defect based on the test results of carburized gears made of SCM420 clean steel, gears with both an artificial notch and nonmartensitic layer at the tooth fillet and so forth. It makes clear the practical use of the presented method, and the strength of carburized gears can be evaluated based on the principal defect size.

Introduction

The high load capacity of carburized gears mainly originates from the hardened layer and induced residual stress. This is the reason that carburization is frequently used as a normal heat treatment for heavy duty gears. One of the authors has clarified the effects of hardness and residual stress on the enhancement of bending fatigue strength and proposed an experimental formula for the estimation of strength (Refs. 1 and 2). The formula was expressed as a function of hardness and residual stress. The effectiveness of the formula has been verified by comparison with many fatigue test results (Ref. 3).

Contrary to the positive effect of carburization mentioned above, the decarburized nonmartensitic layer appears at the tooth surface through the treatment, and this decreases the strength. The authors have observed many microcracks in the nonmartensitic layer and presented a model of fatigue crack propagation. Some cracks are combined when the tooth is loaded and the most critical crack propagates into the deeper region (Ref. 4). Therefore, the nonmartensitic layer should be considered as a defect, which reduces the strength. Besides the nonmartensitic layer, many inclusions such as oxide or sulphur, exist in the hardened layer. Their influence has to be included in the strength evaluation.

Murakami (Ref. 5) proposed a formula to estimate the fatigue strength of a high-strength material from its hardness, stress ratio and the projected area of a defect. It may be used for
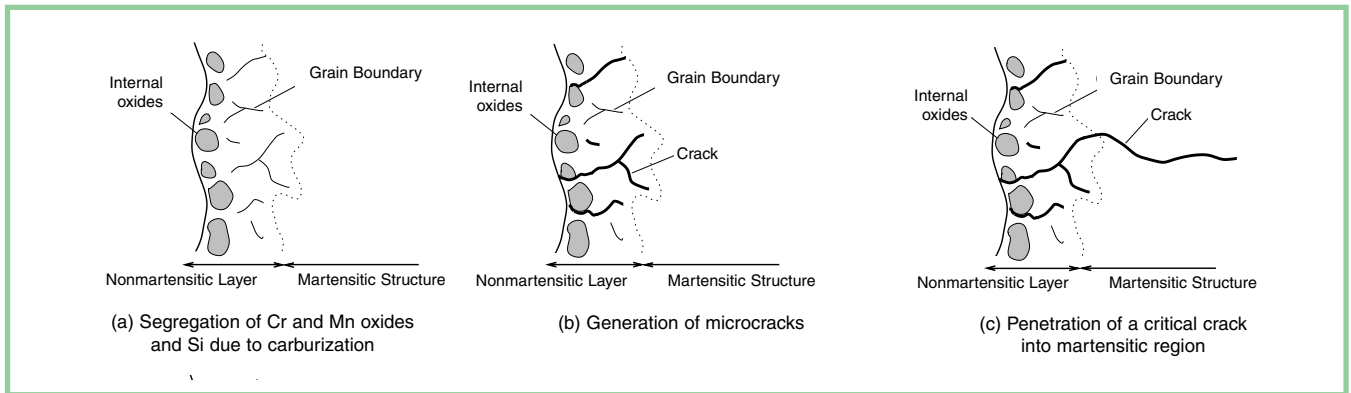
Figure 2—A model of crack initiation mechanism.

the investigation of why the empirical proportionality relationship between fatigue strength and hardness deviates from the relationship in the region of higher hardness (Ref. 6). The formula is also useful for the strength evaluation of carburized gears with latent defects. Quantification of the defects is the key to the derivation of a formula for gears. Therefore, the authors performed a fatigue test using gears with an artificial notch at the fillet, which was processed by focused ion beam, to quantify the influence of the defect in the tooth by this equivalent notch depth (Ref. 7). Another test was also performed to quantify the influence of a nonmartensitic layer, and a formula for the strength of gears with or without nonmartensitic layers was derived using these defect sizes (Ref. 8).

In this paper, the derivation of the formula is briefly reviewed first, and the formula is applied to the fatigue test result of carburized gears made of SCM420 clean steel to demonstrate its wide application. Then, the principal defect, which is substituted for the defect size in the formula to estimate the strength, is inferentially identified so as to evaluate the strength of gears with several kinds of defects, such as inclusions, surface defect and a nonmartensitic layer. This enables use of the formula in a practical gear design and enhancement of the strength. Lastly, the validity of the formerly proposed formula is examined in comparison with the estimation focusing on the defect size.

Derivation of a Formula for Bending Strength Considering the Influence of Defect Size

In order to derive a formula for the evaluation of bending strength of carburized gears, the test gears C1, C2, EP1 and EP2, as shown in Table 1, are used. The material, module and the number of teeth used in the study are low alloy steel SCM415, 5 and 18, respectively. The chemical composition of the alloy is standardized as shown in Table 2.

Carburized gears without nonmartensitic layer. A micronotch is created at the fillet of EP2 gears using a focused ion beam, and the fatigue test is carried out to experimentally determine the threshold notch depth, which is the limit that doesn't reduce the strength of the carburized gear. The notch is at the position where cracks are most frequently initiated in the fatigue test (Ref. 9). The ion beam etching area is rectangular, 500 μm (along face width) x 10 μm, at the center of the face

Table 2—Standard of chemical compositions of material SCM415 (wt%).						
C	Si	Mn	P	S	Cr	Mo
0.13–0.18	0.15–0.30	0.60–0.80	<0.03	<0.03	0.90–1.20	0.15–0.30

width. The desired notch depth is obtained by controlling the time of ion beam irradiation. Figure 1 shows the result of the fatigue test. In this figure, open circles indicate that the tooth is not broken. The open triangle and the closed triangle indicate tooth breaks with and without a notch in the fracture structure, respectively. Teeth with notches of 6 μm or smaller break without the notch in the fracture surface while the teeth with the larger notches break with the notches. Therefore, the threshold notch depth a_{nth} is found to be 6 μm and this quantifies the influence of the defect in the teeth.

The nonmartensitic layer is completely removed in the EP2-type gears. So, the authors assume that the initiation and propagation of cracks of the gears are similar to those of ordinary high strength materials, and fatigue strength can be evaluated by the modification of the following experimental formula (Ref. 5).

Dr. Tomoya Masuyama
is a research assistant of machine intelligence and systems engineering at Tohoku University. His research concentration is on the fatigue strength evaluation of gears based on defects.

Prof. Dr. Katsumi Inoue
is a professor of machine intelligence and systems intelligence at Tohoku University. In addition to engineering design, he specializes on the strength and vibration analysis of power transmission gearing.

Prof. Dr. Masashi Yamanaka *is an assistant professor of machine intelligence and systems engineering at Tohoku University. He performs research into materials and mechanisms of power transmission elements.*

Kenishi Kitamura
was a 2001 graduate of Tohoku Univeristy and currently is an employee of East Japan Railway Co.

Tomoyuki Saito
graduated from Tohoku University in 1998 and currently works at Sumitomo Metal Mining Co.

Table 3—Chemical compositions of material SCM420 (wt%, O:ppm).								
Material	C	Si	Mn	P	S	Cr	Mo	O
Range (JIS G4105)	0.17–0.23	0.15–0.25	0.55–0.90	<0.030	<0.030	0.85–1.25	0.15–0.35	–
Ordinary steel	0.22	0.31	0.84	0.019	0.013	1.21	0.15	8
Clean steel	0.21	0.25	0.85	0.012	0.003	1.18	0.15	5

(a) Ordinary steel gear   (b) Clean steel gear
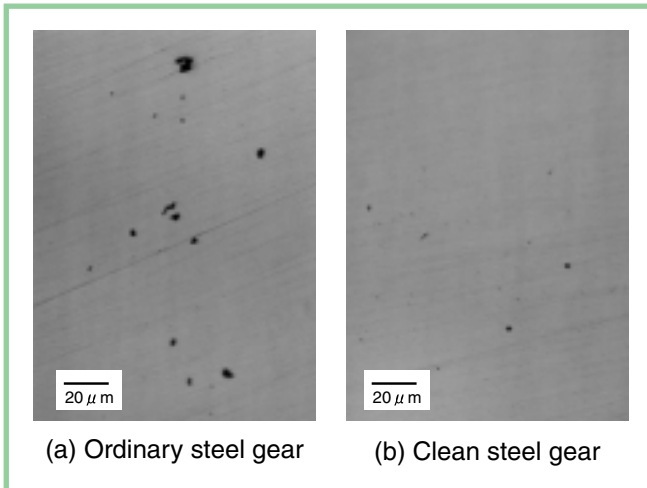
Figure 3—Microstructure of the ordinary steel and clean steel by optical microscope.
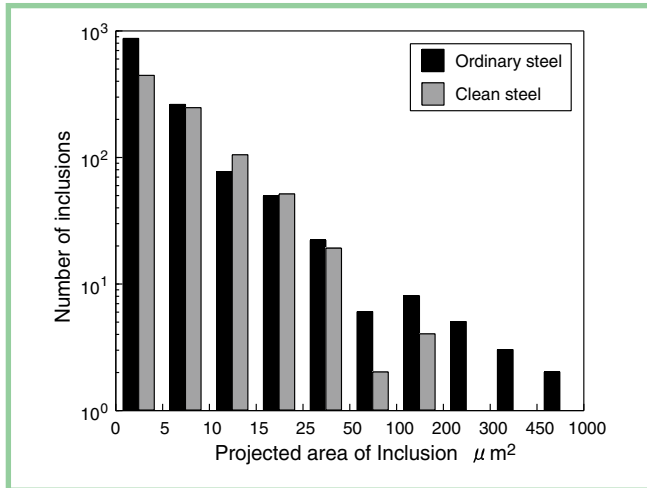
Figure 4—Distribution of inclusions in observed area.
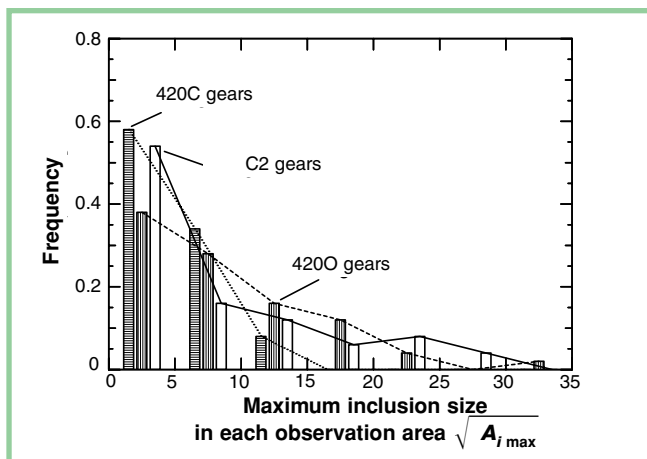
Figure 5—Distribution of the maximum inclusion size in each observed area.

$$\sigma_w = \beta \, \frac{(H + 120)}{(\sqrt{A}\,)^{1/6}} \left[\frac{(1 - R)}{2} \right]^{\alpha} \qquad (1)$$

$$\alpha = 0.226 + H \cdot 10^{-4}$$

Here, σ_w, H and R are fatigue stress amplitude [MPa], Vickers hardness [Hv] and stress ratio, respectively. A represents the projected area of a defect in the direction of the principal stress [μm^2]. The coefficient β is given as $\beta = 1.43$ and may be modified, since the experiment which was the basis of the formula includes few specimens of hard material and few tests subjected to the mean stress.

The formula is applied first to the experimental result of the EP2-type gear. The value of A is assumed to be $\sqrt{A} = \sqrt{10}\, a_{nth}$ since the notch is wide enough to be two-dimensional (Ref. 5) and the stress ratio R is defined assuming that the measured residual stress at the surface, –190 MPa, acts as the mean stress. The strength is estimated at 1,300 MPa and this value is approximately 1.4 times the experimental value of 926 MPa. The estimation error is considerably large, even though the above formula is expected to include approximately ±15% of error (Ref. 5). The coefficient β is therefore modified so that the estimated value agrees well with the strength obtained by the experiment, and the following formula

$$\sigma_w = 0.98 \, \frac{(H + 120)}{(\sqrt{A_i}\,)^{1/6}} \left[\frac{(1 - R)}{2} \right]^{\alpha} \qquad (2)$$

is obtained. The dashed line in Figure 1 shows the strength calculated according to the formula.

It is used for the evaluation of the strength of carburized gears without the nonmartensitic layer. In general, since the threshold notch depth is unknown, we have to find the size of inclusion A_i in the surface layer to substitute it for A in the formula.

For highly reliable design of safety, the worst condition of defect in the gear tooth has to be estimated and substituted for A. The extreme value analysis can be used to estimate the maximum inclusion size in the material (Ref. 5). The authors have applied this analysis to the gear of clean steel and estimated the inclusion size (Ref. 10). However, in this report, we discuss the mean value of gear strength.

Therefore, since the mean size of the defect that determines strength is specified, the average value of the maximum inclusion size contained in each microscope view was substituted into the formula.

Carburized gears with a nonmartensitic layer. The fatigue-loaded C1-type gear is prepared until a crack is detected. The gears were observed using a scanning electron microscope (SEM) and an electron probe microanalyzer (EPMA) to clarify the characteristics of the crack initiation mechanism in the nonmartensitic layer. The test tooth is cut at the center of the face to the normal direction using a cutting wheel. After cutting, the newly produced surface is polished with emery paper and then buff-polished. The obtained surface is etched with 3% nitrate ethanol, then observed by the SEM. In the deeper region, a needle-like martensitic structure is observed. However, at the surface area, there is a layer in which the martensitic structure is not observed. Many microcracks are observed in the nonmartensitic layer, in addition to the cracks which penetrated from the nonmartensitic layer into the deeper region.

The process of crack initiation in a carburized gear tooth with a nonmartensitic layer is considered to be as follows, and the schematic illustrations are shown in Figure 2. In the tooth's nonmartensitic layer before loading, there are Cr and Mn oxides and grain boundaries where Si is segregated (Fig 2a). When subjected to loading, the grain boundaries or oxides act as stress-concentration areas and many microcracks are generated. Some of them combine to form larger cracks (Fig. 2b). The most critical crack is the one that penetrates into the deeper regions while most of the cracks remain in the nonmartensitic layer (Fig. 2c).

As mentioned above, a number of oxides and segregations are distributed in the nonmartensitic layer, and they act as microcracks. Therefore, the nonmartensitic layer should be considered as a defect, which reduces the strength. Here, we assume the thickness of nonmartensitic layer δ is used as the defect size by modifying $\sqrt{A} = \sqrt{10}\,\delta$ and it is substituted for $\sqrt{A}$ in Equation 1. In the case of $\beta = 1.17$, the calculated strengths agree with the experimental results of the three types (C1, C2, EP1) of gears with nonmartensitic layers. Consequently, the following formula is derived.

$$\sigma_w = 1.17 \, \frac{(H + 120)}{(\sqrt{10}\,\delta\,)^{1/6}} \left[\frac{(1 - R)}{2} \right]^{\alpha} \qquad (3)$$

Strength evaluation formula represented by the integrated form. As shown in the above section, we presented two fatigue strength evaluation formulas, Equation 2 and 3, of which coefficients β differ depending on whether the nonmartensitic layer exists or not. In this section, we propose the defect size parameter A', then modify the formula as Equation 4.

$$\sigma_w = \frac{(H + 120)}{(\sqrt{A'})^{1/6}} \left[\frac{(1 - R)}{2} \right]^{\alpha} \qquad (4)$$

Here, the A' is represented as a belong equation.

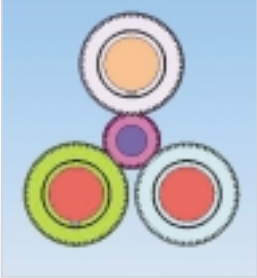When the formula is applied to gears without nonmartensitic layers

(a) Ordinary steel gear   (b) Clean steel gear

Figure 6—Microstructure of the specimen observed by the SEM.

Figure 7—Pulsating fatigue test rig.

Figure 8—S-N curves in 420O gears and 420C gears.

Figure 9—Schematic illustration to infer the principal defect about a carburized gear tooth with an artificial notch.

$$\sqrt{A'} = \frac{\sqrt{A_i}}{0.98^6} \tag{5}$$

$$= 1.13\sqrt{A_i}$$

When the formula is applied to gears with nonmartensitic layers

$$\sqrt{A'} = \frac{\sqrt{10}\,\delta}{1.17^6} \tag{6}$$

$$= 1.23\delta$$

Fatigue Test of Carburized Gears With Defects of Different Sizes

In order to investigate the influence of defects, two types of gears made of SCM420 ordinary steel and SCM420 clean steel were prepared. They were labeled as 420O and 420C respectively. The chemical compositions of these steels are shown in Table 3. The content of oxygen in the clean steel is as low as 5 ppm, and the sulphuric content is also reduced.

Figure 3 shows the optical micrographs at a cross section of both types of gear teeth. Evidently, the clean steel has a few smaller inclusions. It is clearly shown in Figure 4. Though there is no difference in the distribution of inclusion size under $50\ \mu m^2$, in the clean steel gears there are few inclusions greater than $50\ \mu m^2$. In particular, no inclusions greater than $200\ \mu m^2$ were observed. The maximum inclusion size contained in each microscope view was distributed as shown in Figure 5.

The effective case depths of 420O and 420C are 0.92 mm and 0.82 mm, respectively. There was no distinct difference in the hardness distribution. The residual stress σ_R at the root of a tooth was measured by X-ray diffraction method. The residual stress of the clean steel gears is approximately equal to the stress of ordinary steel gears. They are also listed in Table 4. Figure 6 shows SEM micrographs at the fillet of the clean steel gear and the ordinary steel gear. Both of the gears have a similar nonmartensitic layer. In the strength evaluation described later, 15 μm was substituted for thickness of the nonmartensitic layer δ, although the boundary of the nonmartensitic layer is not parallel to the tooth profile.

The fatigue test of the gear is performed using an electrohydraulic fatigue test rig, as shown in Figure 7. The pulsating load is well controlled and the fluctuation of the peak load is less than 2%. The load is applied at a position of 0.5 mm below the tip with the speed of about 40 Hz. To avoid impact loading to the tooth, the stress ratio is set to 0.01. The load is represented by the maximum stress applied at the fillet (Ref. 11).

The S-N curves of the 420O and 420C gears are shown in Figure 8. The test was stopped at $N = 3 \times 10^6$ in each gear and the tooth which was not broken by this lifetime was considered a non-failure. The mean fatigue strengths are obtained as 685 MPa and 650 MPa, respectively, by a staircase method (Ref. 12). The step of stress was 62 MPa.

Since the thickness of the nonmartensitic layer of the two gears is almost identical and the fatigue strength is limited by the nonmartensitic layer, the inclusions did not affect the fatigue
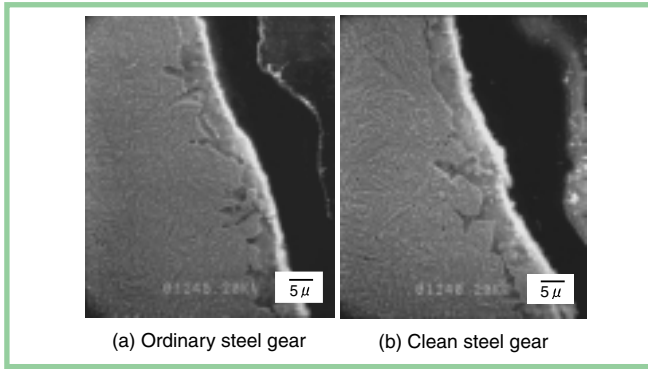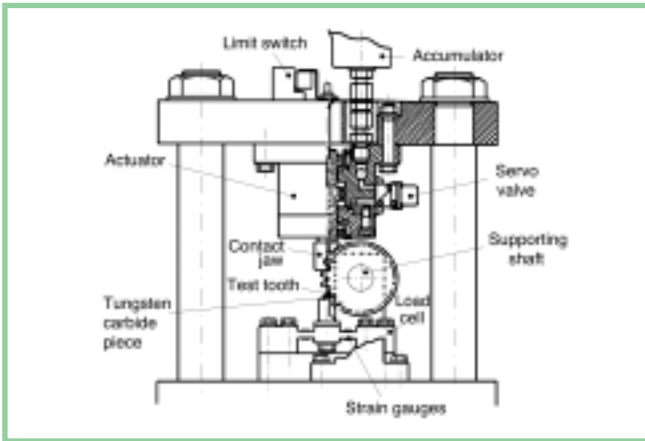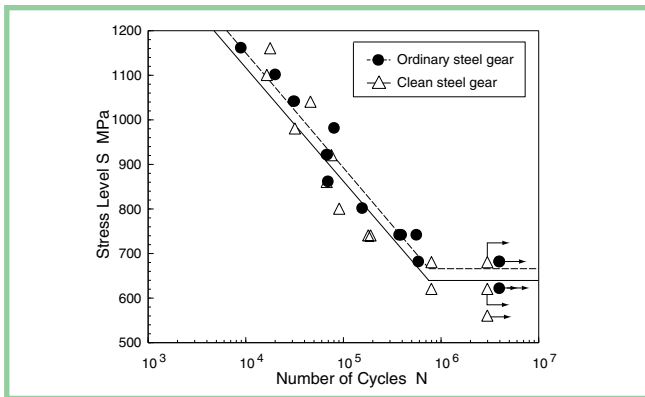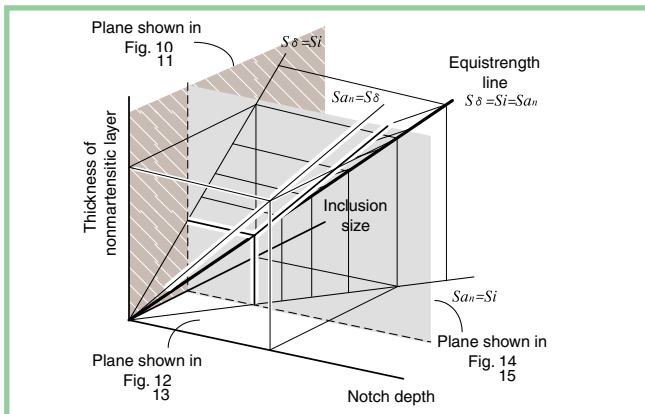
strength. After the removal of the nonmartensitic layer, the fatigue strength increases to 1,070 MPa for clean steel gears and 837 MPa for ordinary steel gears. The fatigue strength enhancement is about 22% and 65%, respectively.

Inferential Identification
of Principal Defect Limiting the Strength

From the viewpoint of defects, the carburized gears for practical use are damaged in the process of steel manufacturing, hobbing and heat treatment. The damage consists of inclusions, tool marks and nonmartensitic layers. In this section, supposing the artificial notch approximates the tool mark, the influences of these defects are discussed to inferentially identify the principal defect which limits the strength.

The proposed formula is used in reverse to evaluate the defect size from the given strength. The relationship among the defects which causes the equal strength is shown in Figure 9, where the top notch depth, inclusion size and nonmartensitic layer thickness are taken as coordinates. Three defects at a point on the line in the space give the equal bending strength. When the hardness and residual stress are constant, A' is equal on the equistrength line.

Inclusion size and thickness of nonmartensitic layers. In the first place, the influences of the inclusion size and the thickness of the nonmartensitic layer are examined. They are illustrated in Figure 9. The line in the figure is the projection of the equistrength line in Figure 10 to the plane of notch depth = 0. Therefore, the nonmartensitic layer acts as the principal defect in the region above the line. The defects of several test gears are plotted in the figure. This shows how the nonmartensitic layer evidently acts as the principal defect in the gears as carburized, and the inclusion becomes tangible after complete removal of nonmartensitic layer. In the case of test gear EP1 electropolished halfway, the remaining nonmartensitic layer seems to be the principal defect, as shown in the figure.

The strengths are estimated based on the defect size mentioned above and compared with the experimental results in Figure 11. The error is about 15% and the inferential identification of principal defect is approximately verified. The fatigue test results of the gears made from spheroidal graphite cast iron FCD700 and FCD950, of which hardness, residual stress and graphite size are H = 330, 280, σ_R = –153 MPa, –92 MPa and A_i = 41.6 μm, 42.2 μm are also shown in this figure. The graphite is considered to be the principal defect in this case, though the error of strength estimation is a bit large, namely 30%.

Figure 10 also suggests a way to enhance the strength. In the case of 420O, for example, the strength increases as the nonmartensitic layer decreases until the thickness is about 4 μm on the curve. The strength is expected to be 970 MPa. Since the clean steel 420C has a small inclusion size, the strength after removing the nonmartensitic layer is expected to be 1,070 MPa. However, more of the nonmartensitic layer should be removed.

Principal defect of gears with an artificial notch on nonmartensitic layer. In the second place, the influences of the notch depth and the inclusion size on the strength of gears

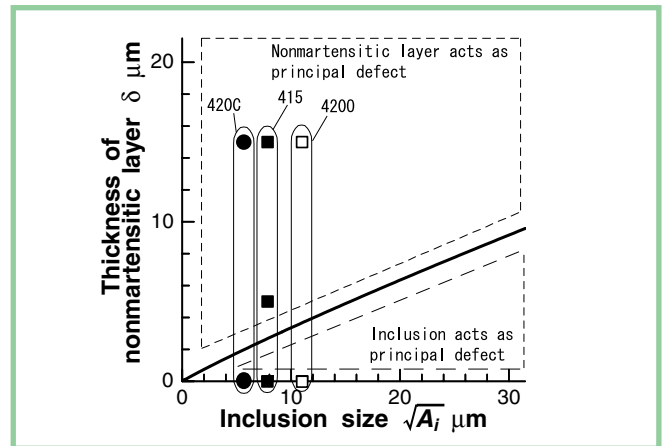| Table 4—Dimensions of test gears.				
Code	420O	420O(EP)	420C	420C(EP)
Material		SCM420 (Ordinary)		SCM420 (Clean)
Module [mm]			5	
Number of teeth			18	
Face width [mm]			8	
Heat treatment			Carburized	
Removal stock [μm]	0	30–40	0	30-40
Hardness [Hv]	628	700	605	702
Residual stress [MPa]	–109	–284	–101	–283
Fatigue strength [MPa]	685	837	650	1,070

Figure 10—Comparison of the influence of the inclusion size and the thickness of nonmartensitic layer.
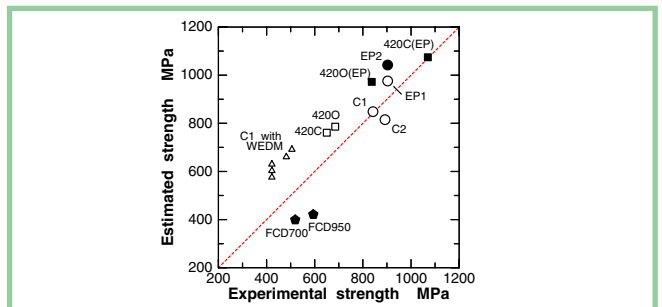

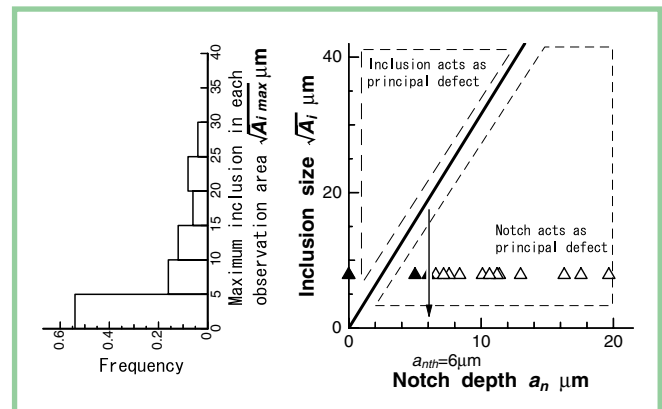*Figure 11—Estimation of strength of gears based on the defect size.*

Figure 12—Comparison of the influence of the notch depth and the inclusion size.

www.powertransmission.com • www.geartechnology.com • **GEAR TECHNOLOGY** • MAY/JUNE 2004 **35**

without nonmartensitic layers are shown in Figure 12. The equistrength line in Figure 9 is projected on this plane, and the inclusion acts as the principal defect in the region above the line. The test results of broken EP2 gears shown in Figure 1 are plotted in the figure. As mentioned before, the closed triangle indicates the notch was not included in the fractured surface. Therefore, an inclusion would act as the principal defect and the plot should be in the region above the equistrength line. Contrary to expectation, there is a plot in the region below the line, and it remains unsolved. As mentioned above, the value of the vertical axis in this evaluation is the average value of the maximum inclusion size in each observed area. The size of inclusion

obtained by the microscopic observation is, however, scattered in a rather wide range as illustrated in the figure. So, the actual size of the inclusion which caused the tooth breakage is not clarified, and this may be the above mentioned result. This figure quantitatively shows the effectiveness of tooth surface finishing in enhancing the strength.

Figure 13 indicates the fatigue test result of C2 gears with an artificial micronotch as well as a nonmartensitic layer. The meaning of marks in the figure is the same as Figure 1. Since the inclusion is comprised in the material, the influences of three kinds of defects are examined in the plane of inclusion size of $A_i = 8.7$ μm in Figure 9. It is illustrated in Figure 14. The region where the inclusion acts as the principal defect is presented by the small area close to the origin and the equistrength line is drawn in the region except for the area shown in the figure. This suggests the inclusion acts as the principal defect, and only in the case of good surface finishing is it experienced. Though numerous tooth breakages, which were not caused by the notch, are plotted in the region below the equistrength line, it remains unsolved.
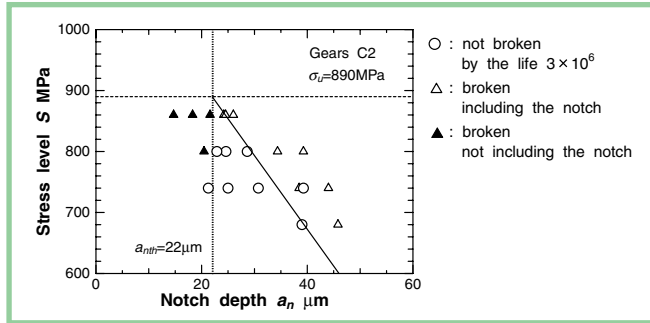

Figure 13—Strength of carburized gear with a micronotch.
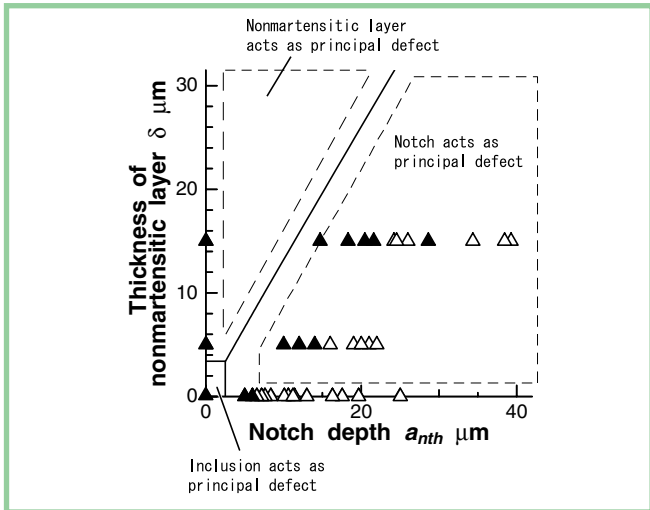

Figure 14—Comparison of the influence of the notch depth and the thickness of the nonmartensitic layer when the inclusion exists.
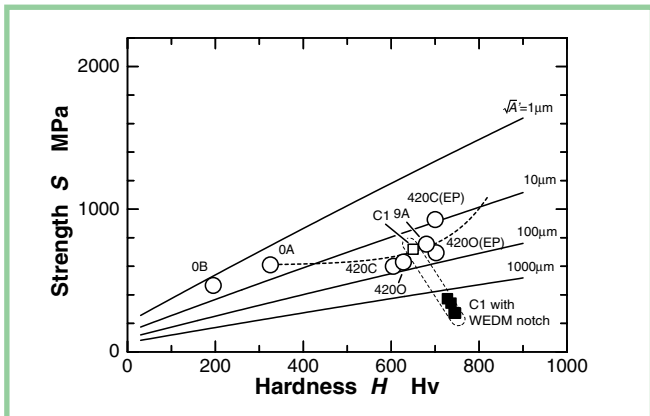

Figure 15—Estimation of strength of gears.

Verification of the Effectiveness of Proposed Formula

The authors have clarified the effects of hardness and residual stress on the enhancement of bending fatigue strength and proposed an experimental formula for the estimation of strength (Refs. 1 and 2). The formula is expressed as

$$
\begin{aligned}
\sigma_u &= \sigma_{uc} + \sigma_{usc} + \sigma_{uR} \qquad (7)\\
&= f(Hc) + g(Hs - Hc) + h(\sigma_R)\\
&= (257 + 1.17Hc) + 3.1 \exp[0.0097(Hs - Hc)]\\
&= -0.5\sigma_R
\end{aligned}
$$

Here, Hc[Hv] is core hardness, Hs[Hv] is surface hardness, σ_R [MPa] is residual stress. Additionally, $\sigma_{uc} = f(Hc)$, $\sigma_{usc} = g(Hs - Hc)$, and $\sigma_{uR} = h(\sigma_R)$ express fatigue strength of the material without heat treatment, increased fatigue strength due to case hardening and fatigue strength due to residual stress, respectively. In the formula, the influence of defects on the strength is not considered.

The strength obtained in Equation 7 is compared with the strength evaluated in Equation 4 in Figure 15, taking the defect size as a parameter. The estimation by Equation 7 is close to the strength of the gears with 30–40 μm defects and has a considerable error in case of the clean steel 420C(EP). It is confirmed from the figure that the formula in Equation 7 can be used for practical gear design except when the gears have such a small defect. In Figure 15, the gears 0A, 0B and 9A were used for the derivation of Equation 7.

The square plots shown in Figure 15 are the strength of C1 gears with a notch processed by wire electric discharge machining. The strength evaluation method proposed in this report is applicable to the gears with an extremely large defect.

Conclusion

In order to establish a strength evaluation method that takes

defects into consideration, the authors had proposed a formula of strength evaluation. In this research, the formula was modified to more general form and the influences of inclusion size, notch depth and nonmartensitic layer thickness were quantitatively clarified based on the fatigue test results of carburized gears made of SCM420 ordinary steel and SCM420 clean steel. The conclusions may be summarized as follows.

The strength evaluation formulas derived from the test of the carburized gear with the artificial micronotch as well as the nonmartensitic layer were unified using the equivalent defect size $\sqrt{A'}$. Its effectiveness was confirmed by the fatigue test result of carburized gears made of SCM420 ordinary steel and SCM420 clean steel.

The principal defect, which limited the strength, was inferentially identified so as to evaluate the strength of gears with several kinds of defects such as inclusions, tool marks and non-martensitic layers.

After removing the surface nonmartensitic layer, the fatigue strength of clean steel gears was 28% greater than that of ordinary steel gears. However, there was no difference in strength in the case when the nonmartensitic layer existed in the surface. These results were explained from the viewpoint of principal defect.

The strength estimated from hardness and residual stress was close to the strength of gears with 30–40 μm defects. ✿

References
1. Toshimi Tobe, Masana Kato, Katsumi Inoue, Isao Morita and Nobuo Takatsu. "Bending Strength of Carburized SCM420H Spur Gear Teeth." *JSME Bulletin*, 29, 1986, pp. 273–280.
2. Katsumi Inoue, Toshiyuki Maehara, Masashi Yamanaka and Masana Kato. "The Effect of Shot Peening on the Bending Strength of Carburized Spur Gear Teeth." *JSME.* 54–502, C, pp. 1331–1337.
3. Katsumi Inoue and Masana Kato. "Estimation of Fatigue Strength Enhancement for Carburized and Shot Peened Gears." *J. Propulsion and Power,* 10–3, 1994, 362–368.
4. Masana Kato, Toshihiko Yamashita, Tomoya Masuyama and Katsumi Inoue. "A Consideration for the Fatigue Crack Initiation of Carburized Gears." 1995, 192–193.
5. Yukitaka Murakami. 1993, *Metal Fatigue: Effects of Small Defects and Nonmetallic Inclusions* (in Japanese).
6. Garwood, M.F. et al. *Correlation of Laboratory Tests and Service Performance, Interpretation of Tests and Correlation with Service.* ASM (1951) 1–77.
7. Tomoya Masuyama, Masana Kato, Katsumi Inoue and Gang Deng. "Bending Strength of Carburized Gear Teeth with a Micro Notch," *Proceedings of the 4th World Congress on Gearing and Power Transmission,* Vol. 3, pp. 1449–1461.
8. Tomoya Masuyama, Masana Kato, Katsumi Inoue, and Toshihiko Yamashita. "Evaluation of Bending Strength of Carburized Gears Based on Quantification of Defect Size in the Surface Layer." *Proceedings of DETC'00*, ASME 2000 Design Enginnering Technical Conferences and Computers and Information in Engineering Conference (2000), DETC2000/PTG-14381 (CD-ROM).
9. Katsumi Inoue, Gang Deng and Masana Kato. 1989, "Evaluation of the Strength of Carburized Spur Gear Teeth Based on Fracture Mechanics," *TransJSME* (in Japanese), 55–514, C, pp. 1488–1493.
10. Katsumi Inoue, Kenichi Kitamura, Masashi Yamanaka, Tomoya Masuyama and Jinichi Asano. *Proc. of the 1st Machine Design and Tribology Division Meeting* in JSME (in Japanese), pp. 73–76.
11. Toshimi Tobe, Masana Kato and Katsumi Inoue, "True Stresses and Stiffness of Spur Gear Teeth," *Proc. Of Fifth World Congress on Theory of Machines and Mechanisms.* 2, pp. 1105–1108.
12. Little, R.E., 1972, *Probabilistic Aspects of Fatigue*, *ASTM STP 511,* pp. 29–42.

Tell Us What You Think . . .
E-mail *wrs@geartechnology.com* to
• **Rate this article**
• **Request more information**
Or call (847) 437-6604 to talk to one of our editors!